Portable pyroelectric electron probe microanalyzer with a spot size of 40 μm

Susumu Imashuku and Kazuaki Wagatsuma

Citation: Review of Scientific Instruments **88**, 023117 (2017); doi: 10.1063/1.4976577
View online: http://dx.doi.org/10.1063/1.4976577
View Table of Contents: http://aip.scitation.org/toc/rsi/88/2
Published by the American Institute of Physics

Portable pyroelectric electron probe microanalyzer with a spot size of 40 μm

Susumu Imashuku[a] and Kazuaki Wagatsuma
Institute for Materials Research, Tohoku University, 2-1-1 Katahira, Aoba-ku, Sendai 980-8577, Japan

(Received 13 November 2016; accepted 2 February 2017; published online 24 February 2017)

We report a method of reducing the spot size of an electron beam in a portable pyroelectric electron probe microanalyzer (EPMA) and its application to on-site microanalysis. An electron beam with a spot size of 40 μm full width at half maximum was achieved by preventing the production of an electric field on the side of a needle tip set on the pyroelectric crystal in the EPMA by coating the side of the tip with an insulating material. This spot size was approximately 10 times smaller than that previously reported. We were able to acquire a line scan profile of a thin copper line sputtered on a silicon substrate using the portable pyroelectric EPMA. The width of the sputtered copper evaluated from the line scan profile (120 μm) corresponded to that from a line scan profile obtained by conventional stationary scanning electron microscope-energy dispersive X-ray spectroscopy equipment. *Published by AIP Publishing.* [http://dx.doi.org/10.1063/1.4976577]

I. INTRODUCTION

An electron probe microanalyzer (EPMA) is a powerful tool for performing the elemental analysis of heterogeneous materials in a micrometer-scale area such as alloys, thin films, minerals, ceramics, fossils, and biological specimens. We previously realized a portable EPMA using a pyroelectric crystal as an electron source to satisfy the rapidly increasing demand for the on-site elemental analysis of, for example, inclusions in steel products, grains in minerals, and aerosols.[1,2] The portable pyroelectric EPMA mainly consisted of a pyroelectric crystal, a small rotary pump, a Peltier device, a 3 V battery, an X-ray detector, and detachable vacuum joints. Changing the temperature of the pyroelectric crystal in vacuum leads to the accumulation of charges on its surface and the generation of a high electric field between the surface of the pyroelectric crystal and the analyte. Residual gas molecules are then field ionized, an electron beam is generated, and electrons are accelerated to the analyte. This phenomenon was discovered by Brownridge.[3] He detected X-rays emitted from a gold foil target adjacent to a pyroelectric crystal of cesium nitrate ($CsNO_3$) by changing the temperature of the pyroelectric crystal at a pressure of 10^{-3} Pa. Since his discovery, pyroelectric crystals have contributed to the miniaturization of X-ray generators,[4–9] electron beam generators,[10–15] ion generators,[14,16] neutron generators,[17–20] X-ray fluorescence measurement setups,[21] X-ray absorption fine structure measurement setups,[22] mass spectrometry,[23] and cathodoluminescence spectrometer[24] because a high-voltage power supply is no longer required.

The average spot size of the electron beam of our portable pyroelectric EPMA was 300 μm full width at half maximum (FWHM) (the minimum spot size was 100 μm FWHM, but the spot size was realized for less than a few seconds).[2] This spot size was achieved by applying an electrical field between an electroconductive needle of gold set on a pyroelectric crystal and the analyte. The spot size was insufficiently small to apply the portable pyroelectric EPMA to on-site microanalysis. For example, the identification of inclusions with a size of more than approximately 50 μm is required for thin steel sheets used for beverage cans because such inclusions can be an origin of fracture during the drawing process. The spot size of the electron beam did not change when we used an electroconductive needle with a sharp tip, indicating that the electric field was produced on the side of the needle tip as shown in Fig. 1(a). Thus, in the present study, we reduced the spot size of the electron beam of the portable pyroelectric EPMA by preventing the production of the electric field on the sides of the needle tip by coating the sides of the tip with an insulating material as shown in Fig. 1(b). After reducing the electron spot size, we demonstrated an application of the portable pyroelectric EPMA to on-site microanalysis.

II. EXPERIMENTAL

A schematic view of the portable pyroelectric EPMA in the present study is shown in Fig. 2(a). A platinum-iridium alloy ($Pt_{0.8}Ir_{0.2}$) wire with a sharp tip was used as an electroconductive needle, which was placed on the $LiTaO_3$ pyroelectric crystal. The sharp tip was fabricated by electrochemical etching of the $Pt_{0.8}Ir_{0.2}$ wire, which had a diameter of 0.3 mm. The electrochemical etching was performed by applying an AC voltage in a saturated sodium chloride (NaCl) solution. A carbon rod was used as the counter electrode. After rinsing with acetone, the $Pt_{0.8}Ir_{0.2}$ wire was immersed in the saturated NaCl solution, and then an AC voltage of 7.5 V was applied between the $Pt_{0.8}Ir_{0.2}$ wire and the carbon rod for 1 s to remove the oxide layer on the $Pt_{0.8}Ir_{0.2}$ wire. After that, the end 1 mm of the $Pt_{0.8}Ir_{0.2}$ wire was submerged in the saturated NaCl solution. An AC voltage of 25 V was applied between the $Pt_{0.8}Ir_{0.2}$ wire and the carbon rod until the current flow became 140 mA. Subsequently, we set the AC voltage to 3 V until the current flow became zero. Then, the etched $Pt_{0.8}Ir_{0.2}$ wire was rinsed with ultrapure water at a temperature of 80 °C. A scanning electron microscope (SEM) image of the obtained

[a]Electronic mail: susumu.imashuku@imr.tohoku.ac.jp

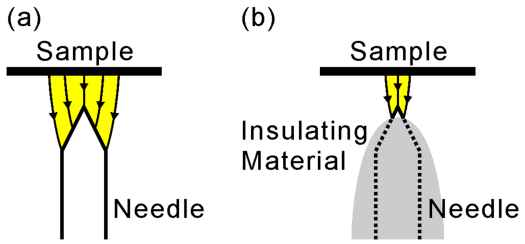

FIG. 1. Schematic diagrams showing an electric field generated between the needle and sample (a) without and (b) with coating the sides of the tip with an insulating material.

$Pt_{0.8}Ir_{0.2}$ wire is shown in Fig. 2(b). The $Pt_{0.8}Ir_{0.2}$ wire with the sharp tip was tightened into a hole on the needle holder with a screw as shown in Fig. 2(c). The $Pt_{0.8}Ir_{0.2}$ wire and the needle holder were covered with epoxy adhesive except for the tip of the $Pt_{0.8}Ir_{0.2}$ wire as shown in Fig. 2(c). The face of the needle holder attached with the screw was only covered

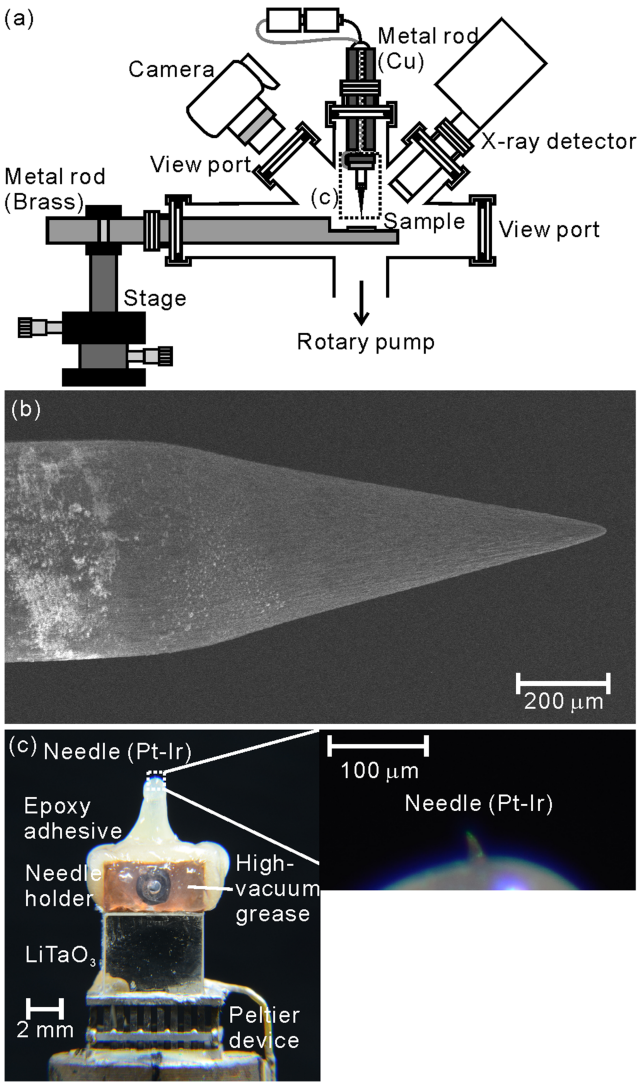

FIG. 2. (a) Schematic view of the portable pyroelectric EPMA presented in this study. (b) SEM image of the tip of a $Pt_{0.8}Ir_{0.2}$ wire after electrochemical etching. (c) Photograph of the electron generation component in the portable pyroelectric EPMA. The photograph on the right shows the picture of the tip of the $Pt_{0.8}Ir_{0.2}$ needle on the pyroelectric crystal.

with high-vacuum grease. We used the epoxy adhesive and the high-vacuum grease to prevent the production of the electric field on the sides of the needle tip and the needle holder. We chose the epoxy adhesive and the high-vacuum grease for this purpose because they are insulating materials and did not decompose at around 130 °C in vacuum. The needle holder was attached to the −z plane of a $LiTaO_3$ crystal with dimensions of 6 mm × 6 mm in the x-y plane and 5 mm in the z-axis. The +z plane of the $LiTaO_3$ crystal was attached to a Peltier device to change the temperature of the $LiTaO_3$ crystal by connecting the Peltier device to a 3 V battery. The other face of the Peltier device was attached to a metal rod using silver paste. A thermocouple was set on the top face of the Peltier device to monitor the temperature of the $LiTaO_3$ crystal. Samples were placed on another metal rod using a carbon tape. The two metal rods were connected with quick-release couplings. The analyzed positions of a sample were controlled with a linear transition manual stage connected to the brass metal rod. The distance between the tip of the $Pt_{0.8}Ir_{0.2}$ wire on the $LiTaO_3$ crystal and the sample was maintained at 2 mm. The pressure of the sample chamber was set to 1 Pa during the measurement using a portable rotary pump. The $LiTaO_3$ crystal was heated to 130 °C for 2 min and then cooled to room temperature. X-ray spectra were measured for 60 s of the cooling cycle with a silicon drift X-ray detector. We also measured the spot size of the electron beam by placing a fluorescent screen (Cu-doped ZnS) on the metal rod connected to the linear transition manual stage. The luminescence of the fluorescent screen was captured with a digital single-lens reflex camera equipped with a close-up lens with a focusing distance of 100 mm through a glass viewport.

III. RESULTS AND DISCUSSION

Figure 3 shows a snapshot of the fluorescent screen during the bombardment of electrons using the portable pyroelectric EPMA. A small area produced green illumination, and the area remained unchanged during the measurement, indicating that the electron beam was successfully focused. The distribution of the brightness of the illuminated area in Fig. 3(a) is shown in Fig. 3(b). The plotted data formed a Gaussian distribution. We then evaluated the spot size of the focused electron beam from the FWHM of the plotted data for three snapshots of the fluorescent screen. The average spot size was calculated to be 40 μm. This value is approximately one-tenth of the spot size we obtained by placing a gold wire on a $LiTaO_3$ crystal.[2] Thus, this result suggests that an electric field was only produced between the needle tip, which was not coated with the insulating material, and the sample (fluorescent screen) as shown in Fig. 1(b). During the electron bombardment on the fluorescent screen, the intensity of the luminescence changed irregularly, indicating that the intensity of the focused electron beam was not constant. This is related to the fact that the cooling rate of the $LiTaO_3$ crystal was not constant because changes in the surface charge density of the $LiTaO_3$ crystal are proportional to its temperature changes.[25] In contrast, the total amount of X-rays generated as a result of bombarding a sample with a focused electron beam during a fixed period did not change when we cooled the $LiTaO_3$ crystal

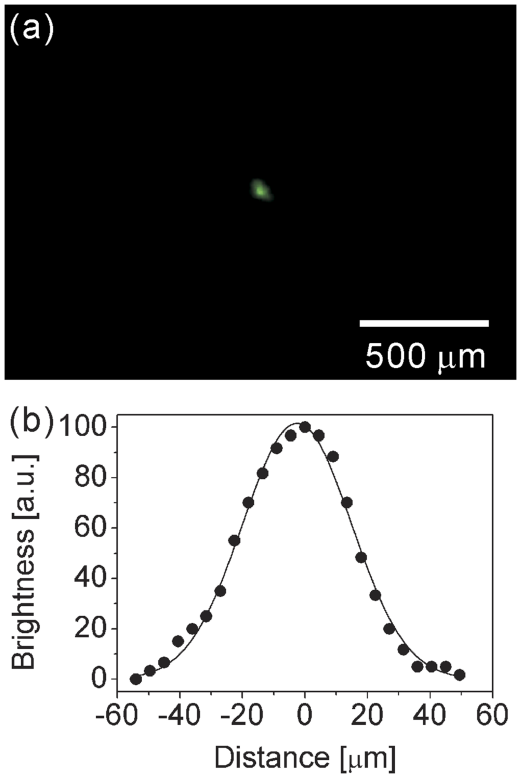

FIG. 3. (a) Photograph of the fluorescent screen during the bombardment of electrons using the portable pyroelectric EPMA. (b) Distribution of brightness of the illuminated area in (a). The fitted Gaussian curve is shown as a solid line.

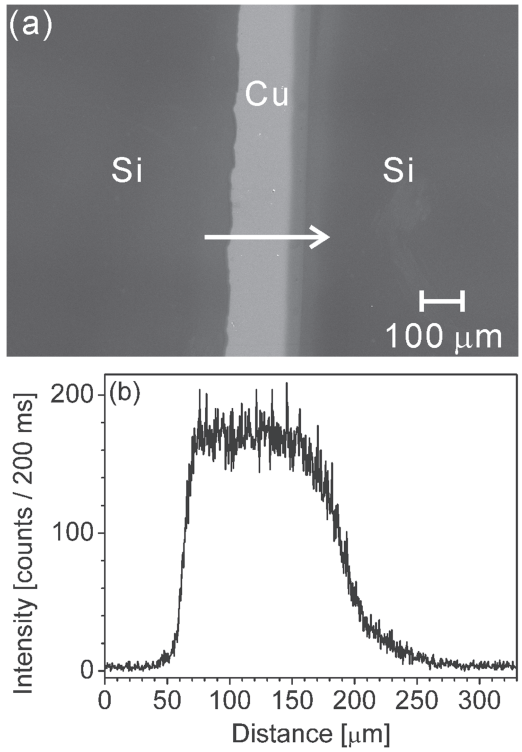

FIG. 4. (a) SEM image of the sample (thin copper line sputtered on silicon wafer). (b) SEM-EDX line scan profile of intensity of Cu Lα line along the arrow in (a).

with the same cooling pattern. Thus, we can obtain reproducible energy dispersive X-ray (EDX) spectra for samples by cooling the $LiTaO_3$ crystal with the same cooling pattern. Actually, the relative standard deviation of the intensity of the Si Kα line was 2.0% when we measured EDX spectra for 60 s five times by bombarding a silicon wafer with the focused electron beam.

We then applied the portable pyroelectric EPMA with the electron beam spot size of 40 μm to the analysis of a thin copper line sputtered on a silicon wafer as shown in Fig. 4(a). The thickness of the sputtered copper was approximately 500 nm. The width of the sputtered copper was 122 μm, which was evaluated from the FWHM of a line scan profile of the Cu Lα line obtained by SEM-EDX analysis (Fig. 4(b)). The copper line was symmetric because the masking on the silicon substrate was not perfect during the sputtering. This evaluated width was in good agreement with that evaluated from a SEM image of the sample (Fig. 4(a)). When the copper sputtered on the silicon wafer was bombarded with the focused electron beam of the portable pyroelectric EPMA, Cu Lα, Si Kα, S Kα, and Cu Kα lines were detected as shown in Fig. 5(a). The characteristic X-rays of copper (Cu Lα and Cu Kα lines) originated from the sputtered copper. The Si Kα and S Kα lines came from the insulating materials of the epoxy adhesive and the high-vacuum grease coated on the $Pt_{0.8}Ir_{0.2}$ wire and the needle holder. These lines were generated as a result of the irradiation of the insulating materials by the continuous and characteristic X-rays emitted from the sample. The energy of the electron beam that bombarded the sample was estimated to be 10 keV because the end-point energy (Duane–Hunt limit) of the continuous X-rays emitted from the sample was 10 keV. Thus, the Si Kα line did not originate from the silicon substrate because the electrons with an energy of 10 keV did not reach the silicon substrate below the sputtered copper with a thickness of 500 nm.[26] When the silicon substrate was bombarded with the focused electron beam of the portable pyroelectric EPMA, Si Kα and S Kα lines were detected as shown in Fig. 5(b). The Si Kα line is attributed to the silicon substrate in addition to the insulating materials coated on the $Pt_{0.8}Ir_{0.2}$ wire and the needle holder because the intensity of the Si Kα line is approximately five times higher than that obtained by bombarding the sputtered copper with the focused electron beam. The S Kα line originated from the insulating materials coated on the $Pt_{0.8}Ir_{0.2}$ wire and the needle holder. It is speculated from the X-ray count rate in Figs. 5(a) and 5(b) that the beam current of the portable pyroelectric EPMA is in nA order. Figure 5(c) shows a line scan profile of the area intensity of Cu Lα line obtained by varying the analyzed positions of the sample using the portable pyroelectric EPMA. The shape of the line profile was similar to that obtained by SEM-EDX analysis: the area intensity of the Cu Lα line drastically increased at the position of 70 μm and then gradually decreased from the position of 160 μm. The intensity of the Cu Lα line around the position of 70 μm was slightly lower than that around the position of 130 μm. In addition, the decay of the area intensity of the Cu Lα line from the position of 160 μm was more gradual than that obtained by SEM-EDX analysis. These differences are related to the different spatial resolutions of the portable pyroelectric EPMA and SEM-EDX. The spatial resolution of the portable pyroelectric EPMA is approximately equal to its spot size of

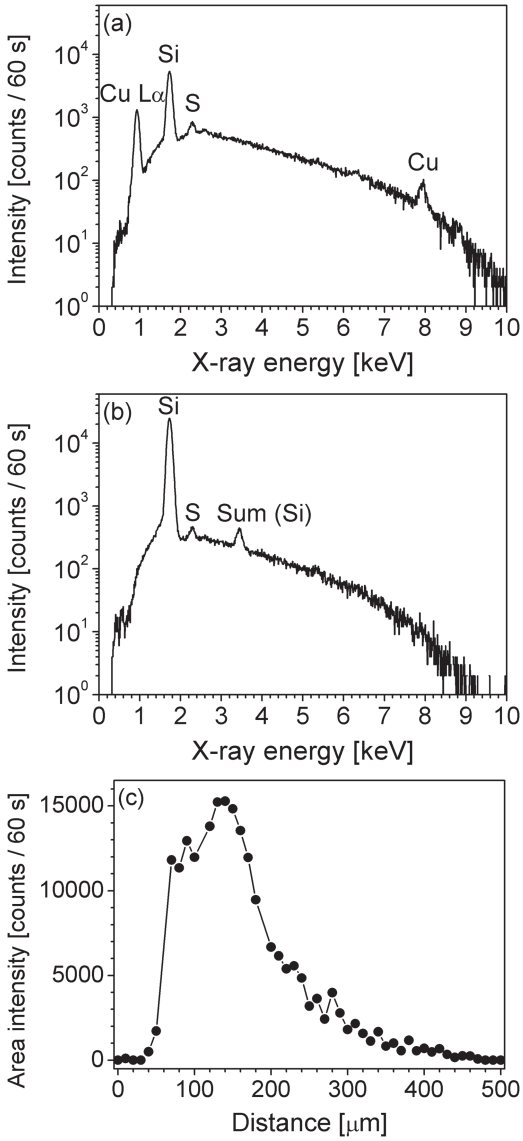

FIG. 5. EDX spectra of the sample obtained at (a) the sputtered copper (at the position of 150 μm in (c)) and (b) the silicon substrate (at the position of 500 μm in (c)) by bombardment with the electron beam using the portable pyroelectric EPMA. (c) EDX line scan profile of area intensity of Cu Lα line obtained using the portable pyroelectric EPMA.

40 μm, whereas that of SEM-EDX is approximately 1 μm. The FWHM of the line scan profile in Fig. 5(c) was estimated to be 120 μm. This value was almost the same as that evaluated from the SEM-EDX line scan profile. Therefore, we were able to obtain a rough line scan profile of the sputtered copper with a width of 120 μm and evaluate its width using the portable pyroelectric EPMA.

IV. CONCLUSIONS

We obtained an electron beam with a 40 μm spot size by placing a $Pt_{0.8}Ir_{0.2}$ wire, whose tip was sharpened by electrochemical etching, on the pyroelectric crystal and coating the sides of the sharp tip with insulating materials. The obtained spot size was approximately 10 times smaller than that without covering the sides of the tip with insulating materials. Utilizing the portable pyroelectric EPMA with the electron beam spot size of 40 μm, we succeeded in acquiring a rough line scan profile of a thin copper line sputtered on a silicon substrate. The width of the sputtered copper evaluated from the FWHM of the obtained line scan profile was 120 μm, which was in good agreement with that evaluated from the FWHM of a SEM-EDX line scan profile of the same sample. The pyroelectric EPMA realized in the present study is extremely portable because it mainly consists of a pyroelectric crystal with an electroconductive needle having a sharp tip, a 3 V battery to operate the Peltier device, an X-ray detector, a portable rotary pump, detachable vacuum joints, and a linear transitional stage. Thus, the portable pyroelectric EPMA is expected to contribute to on-site elemental analysis in microscale areas such as inclusions in steels and grains in minerals.

ACKNOWLEDGEMENTS

We greatly appreciate Professor Naoto Todoroki, Tohoku University, for showing us the method of fabricating a needle with a sharp tip. Financial support for the present study was provided by a Promotion Grant and JSPS KAKENHI Grant No. 26709056.

[1] S. Imashuku, A. Imanishi, and J. Kawai, Anal. Chem. **83**, 8363 (2011).
[2] S. Imashuku, A. Imanishi, and J. Kawai, Rev. Sci. Instrum. **84**, 073111 (2013).
[3] J. D. Brownridge, Nature **358**, 287 (1992).
[4] J. D. Brownridge and S. M. Shafroth, J. Appl. Phys. **85**, 1298 (2004).
[5] J. A. Geuther and Y. Danon, J. Appl. Phys. **97**, 104916 (2005).
[6] E. Hiro, T. Yamamoto, and J. Kawai, Adv. X-ray Chem. Anal. Japan **41**, 195 (2010).
[7] S. Imashuku and J. Kawai, Rev. Sci. Instrum. **83**, 016106 (2012).
[8] Y. Alivov, M. Klopfer, and S. Molloi, Appl. Phys. Lett. **102**, 143106 (2013).
[9] See http://www.amptek.com/ for the information on the portable pyroelectric X-ray generator.
[10] G. Rosenman, D. Shur, Y. E. Krasik, and A. Dunaevsky, J. Appl. Phys. **88**, 6109 (2000).
[11] J. D. Brownridge, S. M. Shafroth, D. W. Trott, B. R. Stoner, and W. H. Hooke, Appl. Phys. Lett. **78**, 1158 (2001).
[12] J. D. Brownridge and S. M. Shafroth, Appl. Phys. Lett. **79**, 3364 (2001).
[13] E. M. Bourim, D.-W. Kim, V. S. Kin, C.-W. Moom, and I. K. Yoo, J. Electroceram **13**, 293 (2004).
[14] J. A. Geuther and Y. Danon, J. Appl. Phys. **97**, 074109 (2005).
[15] M. Hockley and Z. Huang, Appl. Phys. Lett. **101**, 222901 (2012).
[16] M. Hockley and Z. Huang, J. Appl. Phys. **113**, 034902 (2013).
[17] B. Naranjo, J. K. Gimzewski, and S. Putterman, Nature **434**, 1115 (2005).
[18] J. Geuther, Y. Danon, and F. Saglime, Phys. Rev. Lett. **96**, 054803 (2006).
[19] W. Tornow, S. M. Shafroth, and J. D. Brownridge, J. Appl. Phys. **104**, 034905 (2008).
[20] D. Gillich, A. Kovanen, B. Herman, T. Fullem, and Y. Danon, Nucl. Instrum. Methods Phys. Res., Sect. A **602**, 306 (2009).
[21] J. Kawai, H. Ida, and T. Koyama, X-ray Spectrom. **34**, 521 (2005).
[22] S. Mitsuya, H. Ishii, and J. Kawai, Appl. Phys. Lett. **89**, 134104 (2006).
[23] E. L. Neidholdt and J. L. Beauchamp, Anal. Chem. **79**, 3945 (2007).
[24] S. Imashuku, N. Fuyuno, K. Hanasaki, and J. Kawai, Rev. Sci. Instrum. **84**, 126105 (2013).
[25] J. F. Nye, *Physical Properties of Crystals* (Oxford University Press, New York, 1985), p. 78.
[26] J. Goldstein, D. Newbury, D. Joy, C. Lyman, P. Echlin, E. Lifshin, L. Sawyer, and J. Michael, *Scanning Electron Microscopy and X-ray Microanalysis*, 3rd ed. (Springer, New York, 2008), p. 68.